Acta Polytechnica CTU Proceedings **54**:67–71, 2025
https://doi.org/10.14311/APP.2025.54.0067

PRESTRESS LOAD DISTRIBUTION MODELING FOR CONTAINMENT DIGITAL TWIN MODEL

Matyáš Ratislav[a,*], Bořek Patzák[b], Petr Štemberk[a], Jan Štěpán[c]

[a] *Czech Technical University in Prague, Faculty of Civil Engineering, Department of Concrete and Masonry Structures, Thákurova 7, 166 29 Prague 6, Czech Republic*

[b] *Czech Technical University in Prague, Faculty of Civil Engineering, Department of Mechanics, Thákurova 7, 166 29 Prague 6, Czech Republic*

[c] *Institute of Nuclear Research Řež, a. s. Hlavní 130, Řež 250 68, Husinec, Czech Republic*

[*] corresponding author: matyas.ratislav@fsv.cvut.cz

Abstract. This paper examines the prestress load distribution in the ducts of the prestressing tendons of a VVER-type nuclear reactor containment. It introduces a method for distributing the simplified linear load from the prestressing cable onto the surface area of the duct. Furthermore, a procedure for applying this calculation to a detailed numerical 3D model of a containment segment is described. This method can be implemented into computational software, such as OOFEM, to incorporate this more accurately defined load into a comprehensive stress analysis of the segment. Realistic definition of load distribution from prestressing tendons on the surface of the ducts is critical for identifying potential deviations from a uniform prestress distribution within the containment wall. This, in turn, facilitates assessments such as evaluating the extension of the structure's service life.

Keywords: Unbonded prestressing reinforcement, structural loading, prestressing ducts, digital twin, 3D model.

1. Introduction

Containments represent a crucial component of the protective systems in nuclear power plants using VVER nuclear reactors, ensuring safety and integrity in case of emergency situations [1]. These containments are designed as prestressed reinforced concrete structures that utilize prestressing tendons to enhance strength and resilience [2, 3]. The use of a digital twin, which is a virtual model of a physical system, enables analyses and predictions of the behavior of these structures.

The aim of this article is to develop a method for determining the surface load from prestressing on the wall of a tendon duct within a containment segment model. Calculations performed on this detailed model will be used to refine the digital twin, defined in this paper as a numerical model of the entire containment building. Therefore, the precision in defining load distribution from prestress in tendon ducts will directly impact the accuracy of the digital twin. This digital twin will enable improved assessment, prediction, and decision-making in future service-life extension processes for the structure.

The structure of the article is as follows: In the first section, the finite element model and its parameters are presented. Next, the linear load from the prestressing cables is defined. Then, the calculation of the load distribution coefficient is described. Following this, the coordinate transformation for applying the calculations discussed in the previous sections to the aforementioned numerical model of the structure is addressed. Finally, the results and their potential further applications are discussed.

2. Prestress loads in nuclear reactor containment vessels

The determination of prestress loads was conducted for the digital twin model of a segment of a VVER-1000 reactor containment structure. The containment of this reactor is a monolithic, post-tensioned cylindrical reinforced concrete structure, with its walls prestressed by a cable system arranged in cross loops. This prestressing system consists of unbonded tendons arranged in a helical pattern [4, 5].

The modeled segment is a three-dimensional finite element model designed for detailed stress analysis within the containment structure. Although this model has been employed in previous studies [6], it can be enhanced using updated data, advanced methodologies (e.g., new optimization techniques for defining boundary conditions or the approaches discussed in this paper), and improved software tools. The model represents a typical cross-section of the containment structure, intentionally excluding the effects of openings, supports, and the containment ring beam on the stress distribution within this segment. Due to the containment size, creating such a detailed finite element model for the entire containment is impractical as it would result in extremely demanding computations. The chosen segment has a height of 2.12 meters, a thickness of 1.2 meters, and an arc width of 3 meters at its midplane. The model also includes reinforcing

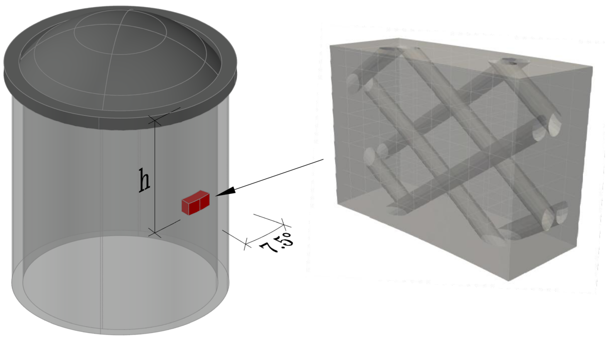

Figure 1. Schematics of numerical model for containment segment.

steel bars represented by 1D elements.

The unbonded post-tensioning tendons are modeled as external loads acting on the inner walls of the post-tensioning ducts, which are represented as cavities within the segment mass (see Figure 1). The curvature of both the segment and the ducts corresponds to the curvature of the entire containment. The finite element mesh comprises tetrahedral elements, with a higher mesh density in the regions adjacent to the inner walls of the ducts. The method of applying the post-tensioning load is crucial for stress development near the ducts, thus special attention was paid to the analysis of load distribution.

2.1. Assessment of line loads

For a detailed determination of the load due to prestressing at any point within the duct, it is first necessary to establish the total line load exerted by the cable along its length on the structure. This line load varies along the length of the cable due to prestress losses and has two components: the first acting in the direction of the axis of the containment cylinder, and the other acting along the direction of the cable (frictional force, which reduces the prestress in the cable) [7].

For the digital twin model, the measurement of prestressing force in the anchorages of the prestressing cables fixed to the containment ring beam can be utilized [8, 9]. The measured force (N_0) can be reduced by losses due to friction up to the point of interest at a distance s from the prestressing location (see Figure 2). From this calculated force in the cable, the line loads can subsequently be determined.

The prestressing force N in the cable at a distance s from the point of prestressing can be determined using the following equation

$$N(s) = N_0 \cdot \exp\left(\frac{-s \cdot \tan(\phi)}{r \cdot (1 + \tan^2(\omega))}\right), \qquad (1)$$

where N_0 is the force at the prestressing location, $\tan(\phi)$ is the friction coefficient, r is the radial distance of the cable from the containment axis, and ω is the vertical cable inclination [7].

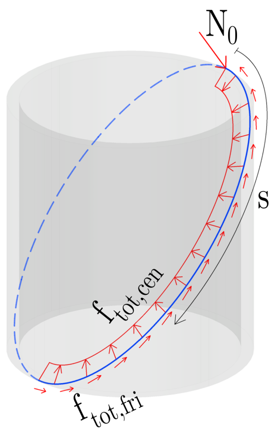

Figure 2. Schematic of line load from prestressing on containment structure.

This calculation is based on the parametrization of prestressing cable paths (helix) along the arc. The line load from the prestressing cable (for detailed explanation see [7]) acting in the radial direction to the containment center (along the internal normal) is given by

$$f_{\text{tot,cent}} = \frac{N(s)}{r \cdot (1 + \tan^2(\omega))}. \qquad (2)$$

The line load acting in the direction of the prestressing cable (tangent to the cable axis) is

$$f_{\text{tot,fri}} = f_{\text{tot,cent}} \cdot \tan(\phi). \qquad (3)$$

For graphical representation of these loads, see Figure 2.

2.2. Load distribution on duct surface

In the previous chapter, the duct was considered as a 1D element defined solely by its centerline. To define the magnitude of the load on the duct surface, the linear load calculated according to the procedure described above must be multiplied by a load distribution coefficient within the duct, denoted as ξ. This coefficient ensures the distribution of the linear load over the surface of the duct.

The coefficient ξ depends on the angle μ – the deviation of the normal to the duct surface at the investigated point from the normal to the plane of the structure (i.e., the direction towards the center of the containment), see Figure 3. Since it is assumed that the load acts only on parts of the inner surface of the duct, the coefficient ξ takes non-zero values only within the interval μ belonging to $(-90°, 90°)$. To maintain the calculation for the simplified 1D cable, it must for duct radius r_d hold that:

$$r_d \cdot \int_{-90°}^{90°} \xi(\mu)\, d\mu = 1. \qquad (4)$$

The determination of the load distribution – i.e., the function $\xi(\mu)$ – was based on the assumed distribution

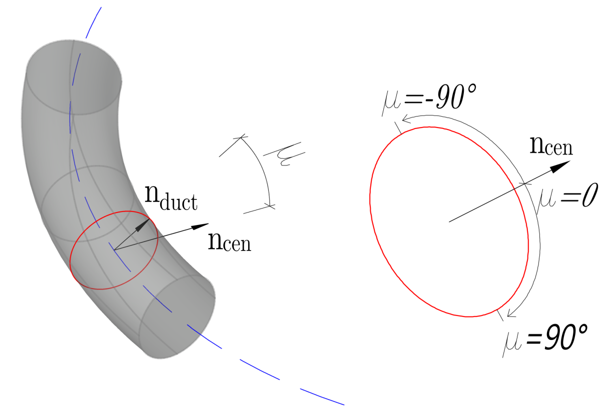

Figure 3. Schematic of μ angle definition.

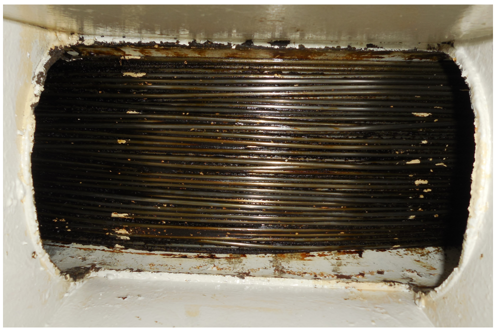

Figure 4. Ilustrative photograph showing bend of unbounded prestressing cable.

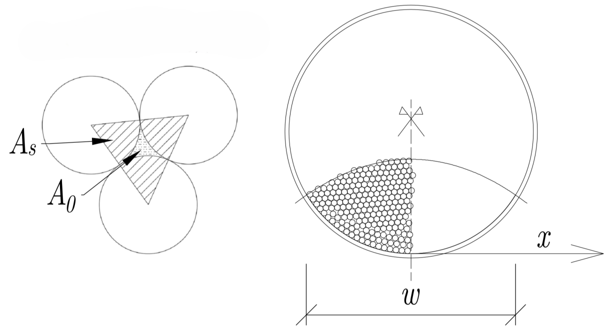

Figure 5. Graphical basis for η estimation.

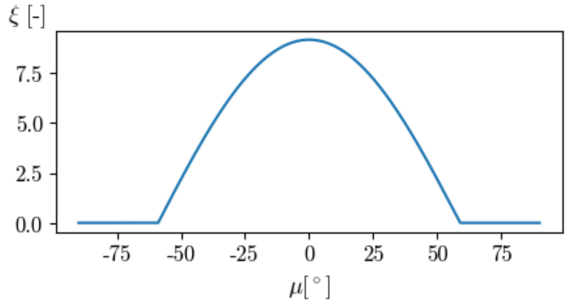

Figure 6. Example of load distribution in tendon duct.

of reinforcement within the duct. It is assumed that the non-bonded prestressing reinforcement will be pressed as much as possible against the inner side of the bend (neglecting the influence of the cable self weight on its distribution). The individual wires will be densely packed, and although the prestressing system considered does not involve individual wires being twisted into a complete cable, it is assumed that due to slight twisting of the wire bundle during installation, the wires will tend to stay more packed together.

It can thus be considered that the distribution of wires within the duct will resemble the shape of an ellipse or a lens. This shape can be simplified to a lens, with one side formed by a circular segment (representing the wall of the duct) and the other side by a parabola. The parameters of the parabola can be defined from the known width of the wire bundle distribution within the duct and the area enclosed by the shape. The width of the bundle w was estimated based on a visual assessment from a photograph of the bend in cylindrical cables (refer to Figure 4). The area of the wire bundle was calculated as the cross-sectional area of the wires multiplied by the coefficient η, which accounts for the space between the wires.

The coefficient η for the densest possible arrangement of wires is 1.102. This value was determined graphically as the ratio of the total area $A_s + A_0$ to the area of the circular prestressing wires A_s in the tightest configuration, see Figure 5. Due to the shape of the duct and the twisting of the bundle, the arrangement will be more relaxed, and η will therefore be higher – the coefficient η was estimated graphically as 1.15. The graphical solutions were performed for a tube with a diameter of 225 mm and 450 wires. The parameters a and b of the parabola can be determined from the following equations

$$2 \cdot \int_0^{w/2} (f_p(x) - f_d(x))\, dx = A_p \cdot \eta, \qquad (5)$$

$$\text{for } x = w/2 : \quad f_p(x) = f_d(x), \qquad (6)$$

where the parabola function is $f_p(x) = ax^2 + b$, the duct function is $f_d(x) = r_d - \sqrt{r_d^2 - x^2}$, A_p is the area of the prestressing reinforcement, and x is as shown in Figure 5. Neglecting the self-weight of the wires, the wire distribution is symmetrical, and it is therefore possible to integrate over only half of the figure.

Assuming that the distribution of the function $\xi(\mu)$ is similar to the distribution of the prestressing wires, it can be defined for the angle of deviation μ as follows

$$\xi(\mu) = \frac{f_p(x(\mu)) - f_d(x(\mu))}{2r_d \cdot \int_0^{\alpha} (f_p(x(\mu)) - f_d(x(\mu)))\, d\mu}, \qquad (7)$$

where $x = r_d \sin(\mu)$ and $\alpha = \arcsin(w/(2r_d))$. An example of the ξ distributionin is shown in Figure 6.

2.3. Coordinate transformation for segment model

To define the load from the prestressing cables at point p with coordinates $X_g = \{x_g; y_g; z_g\}$, which lies on the surface of the ducts in the presented model,

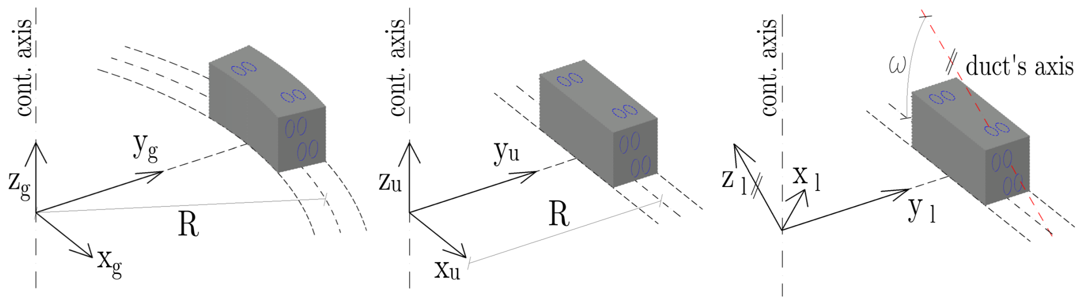

Figure 7. Schematics of employed coordinate systems.

several steps are necessary. This process involves coordinate transformation, the calculation of resulting loads, and their subsequent transformation back to global coordinates.

First, the input global coordinates X_g must be transformed into the coordinates of the developed model X_u, and subsequently transformed into the local coordinates of the duct X_l, on whose surface the investigated point is located. These coordinate systems are schematically depicted in Figure 7.

The transformation from global coordinates X_g to coordinates in the unwrapped coordinate system X_u is defined by the following relationships

$$X_u = \begin{Bmatrix} \operatorname{atan}\left(\frac{x_g}{y_g}\right) \cdot R \\ \sqrt{x_g^2 + y_g^2} \\ z_g \end{Bmatrix}. \tag{8}$$

The transformation from coordinates X_u to the local coordinates of the duct X_l is defined as follows

$$X_l = T \cdot X_u = \begin{bmatrix} \sin(\omega) & 0 & \cos(\omega) \\ 0 & 1 & 0 \\ -\cos(\omega) & 0 & \sin(\omega) \end{bmatrix} \cdot X_u, \tag{9}$$

where ω is the vertical inclination of the ducts.

To perform the calculation, it is further necessary to determine the position c on the duct axis where a cut made by a normal plane will intersect the investigated point. For this purpose, it is required to know the global coordinates of any point on this axis. The coordinates of the mentioned point are converted to local coordinates in the same manner as for point p. These coordinates differ from the coordinates of point c only in the local coordinate z, which is equal to z_l of point p and is thus already known from the previous calculation.

The height of point c in the global coordinate system is obtained as follows

$$z_{g,c} = x_{l,c} \cdot \cos(\omega) + z_{l,c} \cdot \sin(\omega). \tag{10}$$

The input for calculating the line load is the distance s (as given in the Equations 2 and 3). This distance can be obtained as:

$$s = \frac{h - z_{g,c}}{\sin(\omega)}. \tag{11}$$

If $y_{l,p} \leq y_{l,c}$, then for computing the load distribution coefficient ξ, the angle μ is required (else $\xi = 0$ as discussed earlier), which can be calculated as

$$\mu = \operatorname{atan}\left(\frac{x_{l,p} - x_{l,c}}{y_{l,p} - y_{l,c}}\right). \tag{12}$$

After determining the load magnitude from Equations 2 and 3) and multiplying it by the coefficient ξ (acquired via Equation 7), it is necessary to transform the results back to the global coordinate system. See the following equations

$$f_u = T^T \cdot \begin{bmatrix} 0 \\ -f_{\text{tot,cent}} \cdot \xi \\ f_{\text{tot,fri}} \cdot \xi \end{bmatrix}, \tag{13}$$

$$f_g = \begin{bmatrix} y_{g,p}/y_{u,p} & x_{g,p}/y_{u,p} & 0 \\ -x_{g,p}/y_{u,p} & y_{g,p}/y_{u,p} & 0 \\ 0 & 0 & 1 \end{bmatrix} \cdot f_u. \tag{14}$$

3. Conclusion

This study provides a detailed analysis of prestress loads in the containment structure of a VVER-1000 nuclear reactor for use in a finite element 3D model. The results obtained, which include a reasonably precise determination of the surface loading by prestressing cables at any point on the duct surface based on its global coordinates (see Figure 8), contribute to a better understanding of the stress distribution within the structure. The determination was based on engineering estimates informed by observations of actual constructions. The presented computational approach can be effectively implemented in software programs such as OOFEM, facilitating its practical application in the detailed examination of such structures.

Subsequent steps will involve incorporating the prestress loads into the presented model, which will also account for additional acting loads. A comprehensive stress analysis of these combined loads will then enable a more accurate identification of potential deviations from a uniform prestress distribution within the containment wall. The results of this analysis will contribute to the precision of the containment digital twin model, which is used to evaluate the extension of the containment lifespan.

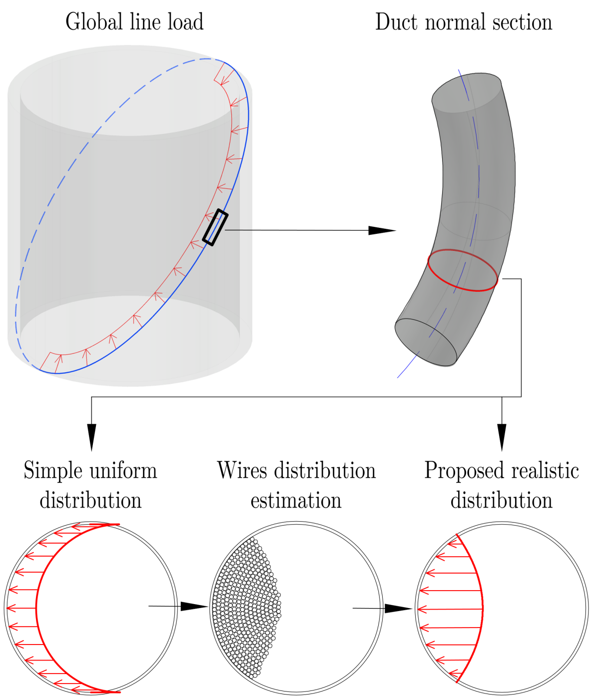

FIGURE 8. Schematics of load evaluation process and illustrative comparison of simplified and refined load distribution.

ACKNOWLEDGEMENTS

The presented work has been realized within Institutional Support by Ministry of Industry and Trade of the Czech Republic and the CTU in Prague project SGS24/038/OHK1/1T/11.

REFERENCES

[1] International Atomic Energy Agency. *Design of the Reactor Containment and Associated Systems for Nuclear Power Plants*. IAEA Safety Standards Series No. SSG-53. IAEA, Vienna, 2019.

[2] Z. Janda, J. Zeman, J. Šejnoha. Zjednodušené modely interakce volného přepínacího kabelu s konstrukcí [In Czech; Simplified interaction models of unbounded tendon with structures]. *Stavební obzor* **18**(2):44–48, 2009.

[3] Nuclear containments. Tech. Rep. 13, fib (International Federation for Structural Concrete), 2001. [2024-07-30]. `https://doi.org/10.35789/fib.BULL.0013`

[4] D. Tonarová, P. Brabec, Z. Fencl, et al. Hodnocení předpínacích kabelů vyjmutých z kontejnmentu ETE [In Czech; Evaluation of prestressed cables removed from NPP Temelín containment]. In *Zvyšování životnosti komponent energetických zařízení v elektrárnách*. ÚJV Řež, a. s., ÚJV Řež, a. s., Výzkumný a zkušební ústav Plzeň s.r.o., ČVUT v Praze, Fakulta strojní, ČEZ, a. s., ZČU v Plzni, Fakulta strojní, RTI, 2019.

[5] P. Rericha, J. Sejnoha. Partial service life assessment of a reactor containment. *Nuclear Engineering and Design* **235**(23):2451–2462, 2005. `https://doi.org/10.1016/j.nucengdes.2005.06.010`

[6] Z. Bittnar, J. Šejnoha, T. Koudelka, et al. JE Temelín, ZS1020 – Opatření pro dlouhodobý stabilní a akceptovatelný provoz ochranných obálek JE Temelín [In Czech; NPP Temelín, ZS1020 – measures for the long-term stable and acceptable operation of the containment structures of the Temelín NPP].

[7] T. Krejčí, J. Šejnoha. Prognóza ztrát předpětí v kabelech válcové části ochranné obálky JETE [In Czech; Prediction of prestress losses in the cables of the cylindrical part of the containment structure of the NPP Temelín]. Tech. rep., České vysoké učení technické v Praze, Fakulta stavební, Katedra mechaniky, Praha, 2003.

[8] State Office for Nuclear Safety. Národní hodnotící zpráva České republiky pro účely topical peer-review „Řízené stárnutí“ dle směrnice o jaderné bezpečnosti 2014/87/EURATOM [In Czech; National assessment report of the Czech Republic for the topical peer review on “ageing management” under the nuclear safety directive 2014/87/EURATOM], 2017.

[9] P. Anderson. Thirty years of measured prestress at swedish nuclear reactor containments. *Nuclear Engineering and Design* **235**(21):2323–2336, 2005. `https://doi.org/10.1016/j.nucengdes.2005.04.002`